Heliyon 9 (2023) e13522

Contents lists available at ScienceDirect

Heliyon

journal homepage: www.cell.com/heliyon

Research article

Solvent-free mechanochemical multicomponent preparation of 4H-pyrans catalyzed by $Cu_2(NH_2\text{-}BDC)_2(DABCO)$ metal-organic framework

Zahra Akhlaghi [a], Mohammad R. Naimi-Jamal [a,*], Leila Panahi [a], Mohammad G. Dekamin [b], Bahareh Farasati Far [a]

[a] *Research Laboratory of Green Organic Synthesis and Polymers, Department of Chemistry, Iran University of Science and Technology, Tehran 16846-13114, Iran*

[b] *Pharmaceutical and Heterocyclic Compounds Research Laboratory, Department of Chemistry, Iran University of Science and Technology, 16846-13114 Tehran, Iran*

ARTICLE INFO

Keywords:
Solvent-free
Ball milling
Mechanochemical
Metal-organic framework
4H-pyrans
Heterogeneous catalyst

ABSTRACT

4H-pyrans have been prepared through a mechanochemical multicomponent reaction (MCR) of different aldehydes, malononitrile, and various 1,3-dicarbonyl compounds, catalyzed by an amine-functionalized metal-organic framework (MOF) $Cu_2(NH_2\text{-}BDC)_2(DABCO)$ as a heterogeneous catalyst with good to excellent yields.

1. Introduction

Pyrans are non-aromatic heterocyclic six-membered rings with a molecular formula of RC_5H_6O, including five carbon atoms, one oxygen atom, and two double bonds. The two isomers of the pyrans differ in the double bond position. In 2*H*-pyran (1), saturated sp3 carbon is positioned at position 2, but in 4H-Pyran (2), it is at position 4 (Scheme 1). In 1962, 4H-pyrans were created for the first time through the thermal decomposition of 2-acetoxy-3,4-dihydro-2*H*-pyran, and their properties and applications were investigated [1,2].

Heterocyclic compounds, including tetrahydrobenzo[b]pyrans and their derivatives, have been studied for their potential medicinal and pharmacological applications (see, for example, Scheme 2) [3]. They have attracted special attention, which can be attributed to their antioxidant [4], anticancer [5], antitumor [6] properties, *etc*. Tetrahydrobenzo[b]pyran-based compounds possess the potential for physical enhancers in treating neurological diseases such as Alzheimer's and Parkinson's diseases, Dawson's syndrome, amyotrophic lateral sclerosis, Huntington, Schizophrenia, AIDS-associated dementia, and myoclonus [7]. Also, these compounds are widely used in cosmetics and as pigments [8].

Various methods have been reported to prepare tetrahydrobenzo[b]pyrans and their derivatives. Generally, the basis of their synthesis is the three-component condensation of variable 1,3-dicarbonyl derivatives, CH-active compounds, and aldehydes. Various heterogeneous and homogeneous catalysts have been reported so far for this condensation reaction, including magnetite L-proline [9], DABCO-CuCl complex [10], trisodium citrate [11], cesium carbonate [12], ninhydrin [13], ionic liquids based on choline hydroxide

---

* Corresponding author.
E-mail address: naimi@iust.ac.ir (M.R. Naimi-Jamal).

https://doi.org/10.1016/j.heliyon.2023.e13522
Received 11 October 2022; Received in revised form 27 January 2023; Accepted 1 February 2023

$[Ch]^+[OH]^-$ [14] or DABCO $[H_2\text{-DABCO}][H_2PO_4]_2\}$ [15], starch solution [16], sulfonic acid functionalized silica [17], $Fe(ClO_4)_3/SiO_2$ [18], ClO_4^-/Al-MCM-41 [19], poly(4-vinyl pyridine) (P4VP) [20], and silica-supported dodeca-tungstophosphoric acid DTP/SiO_2 [21]. These methods may have disadvantages and problems, including using complex, toxic and destructive catalysts, tedious and challenging purification processes, low efficiency, and slow reaction rates.

Crystalline compounds are known as metal-organic frameworks (MOFs), composed of inorganic moieties (metal ions/clusters) and organic linkers, creating a porous structure of different dimensions (Scheme 3) [22]. They have a low density, a large surface area, and a high proportion of catalytically active transition metals. Most often, metals in the lattice of MOFs act as Lewis acids. The solvent type, solvent concentration, opposite ion nature, metal-to-ligand ratio, metal quadratic geometry, pH, temperature, and the nature of guest molecules determine the MOF structure [22–28]. MOFs have many applications in drug delivery, sensors and luminescence, gas separation and storage, and catalytic reactions [29–40].

Mechanochemical reactions are considered nowadays as green methods of chemical synthesis. Among the others, ball-milling has been a widely accepted tool for solvent-free mechanochemical reactions in recent years. The ball milling method has numerous benefits over other procedures, including quick reaction times, solvent-free settings, high yields, and high atom efficacy [41]. Based on successful organic synthesis through ball milling in previous studies [42], Herein, we presented a three-component, solvent-free synthesis of 4H-pyrans derivatives using ball-milling with nanoporous $Cu_2(NH_2\text{-BDC})_2(DABCO)$ as a heterogeneous catalyst with good to excellent yields (Scheme 4). These kinds of reactions can be considered as a base-catalyzed as well as an acid-catalyzed reactions. We have chosen $Cu_2(NH_2\text{-BDC})_2(DABCO)$, to have a bifunctional catalyst, namely both a Lewis acid Cu^{2+}, as well as Lewis base NH_2 in a unique catalyst. The better activity of this catalyst has been shown in comparison to other catalysts.

2. Experimental section

2.1. *Materials and reagents*

All chemicals, such as 2-aminoterephthalic acid (NH_2-BDC), 1,4-diazabicyclo[2.2.2]octane (DABCO), metal salt $Cu(OAc)_2.H_2O$, aldehydes, and 1,3-dicarbonyl components were obtained through Sigma-Aldrich and Merck companies in reagent grade for direct use without additional purification. As eluents, EtOAc and n-hexane (1:1 or 1:2) were used for thin-layer chromatography (TLC).

2.2. *Instrumental*

Melting points have been measured using open capillaries (sealed at one end) using an Electrothermal 9100 instrument. FT-IR spectra were collected using a Shimadzu 8400S spectrometer. Spectra of ^{1}HNMR were obtained using a Bruker 500 MHz spectrometer. DMSO-d_6 was used as solvent at ambient temperature. Using an X'pert MPD, XRD observations were conducted. Philips diffractometer with Cu radiation source ($\lambda = 1.54050$A) operating at 40 mA and40 KV. A MM400 Retsch ball milling device with two 10 mL jars and 7 mm stainless steel balls was utilized at a frequency of 28 Hz.

2.3. *Synthesis of $Cu_2(NH_2\text{-BDC})_2(DABCO)$*

With a molar ratio of 2:2:1, 0.6 mmol of $Cu(OAc)_2.H_2O$, 0.6 mmol of NH_2-BDC, and 0.3 mmol of DABCO were forcefully grinded through solvent-free ball-milling (28 Hz) at ambient temperature for 2 h. This resulted in a green product washed three times with DMF (3 × 10 mL). Methanol was used for solvent exchange three times (10 mL each) at ambient temperature. In order to eliminate methanol molecules, the obtained powdered MOF was heated at 130 °C under a vacuum for 12 h [42].

2.4. *Preparation of 2-amino-3-cyano-4H-pyran derivatives (5, 6, 8, or 9) zcatalyzed by $Cu_2(NH_2\text{-BDC})_2(DABCO)$*

In order to synthesize 2-amino-3-cyano-4H-pyran derivatives (**5**, **6**, **8**, or **9**), a mixture of malononitrile (1 mmol), $Cu_2(NH_2\text{-BDC})_2(DABCO)$ (0.04 g), 1,3-dicarbonyl components (1 mmol), and aldehyde (1 mmol) was grinded through ball-mill forcefully at 27 Hz, at ambient temperature and solvent-free for the indicated intervals. After the reaction (monitored by TLC) was complete, the catalyst was separated by filtration, washed with (hot) ethanol, and dried for reuse. The product was obtained in pure form after evaporation of EtOH or recrystallization, if necessary.

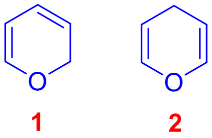

Scheme 1. 2*H*-Pyran and 4*H*-Pyran.

3. Results and discussion

3.1. *Synthesis and characterization of $Cu_2(NH_2\text{-}BDC)_2(DABCO)$*

Following the previously reported procedure, a combination of DABCO, copper (II) acetate, and 2-aminoterephthalic acid in a molar ratio of 1:2:2 was grinded using a ball mill at ambient temperature without the use of any solvent to produce the metal-organic framework Cu_2 $(NH_2\text{-}BDC)_2(DABCO)$ [42] (Scheme 5). The synthesis was finished in less than 2 h, yielding a green powder. Various methods were used to characterize the resultant MOF, including X-ray diffraction (XRD) and Fourier transform infrared spectroscopy (FT-IR).

The as-synthesized XRD pattern of $Cu_2(NH_2\text{-}BDC)_2(DABCO)$ is shown in Fig. 1a,b. The significant peaks at 2θ values of 8, 9, 11, 12, and 16 align well with the previously reported data [42]. Comparing the patterns demonstrated the successful synthesis of a pure $Cu_2(NH_2\text{-}BDC)_2(DABCO)$.

To describe the vibrational modes of the MOF, FT-IR spectroscopy was performed. Fig. 2 depicts the FT-IR spectrum of $Cu_2(NH_2\text{-}BDC)_2(DABCO)$, NH_2-BDC, and DABCO. The asymmetric COO stretch mode (ν_{as}) is observed at 1614 cm^{-1}, whereas CO symmetric stretching is observed at 1377 cm^{-1}. The absorption bands at 3359 and 3469 cm^{-1} correspond to two NH stretching bands of $-NH_2$ groups.

The average particle size of the synthesized $Cu_2(NH_2\text{-}BDC)_2(DABCO)$ samples were determined to be less than 100 nm based on scanning electron microscopy (SEM) images. (Fig. 3a). Transmission electron microscopy was utilized to examine the morphology of $Cu_2(NH_2\text{-}BDC)_2(DABCO)$ (TEM). As depicted in Fig. 3b nano-scaled and crystalline material was generated. It is also important to note that the ball milling approach produced nanoparticles with the consistent distribution. As seen in the TEM photos, the presence of square units indicates the production of $Cu_2(NH_2\text{-}BDC)_2(DABCO)$ frameworks, consistent with the SEM images confirming the nano-cubic shape. Cu was detected in the particles of $Cu_2(NH_2\text{-}BDC)_2(DABCO)$ using energy dispersive X-ray spectroscopy (EDS) (Fig. 3c).

TGA was used to examine the thermal breakdown of $Cu_2(NH_2\text{-}BDC)_2(DABCO)$ at temperatures up to 500 °C at a heating rate of 10 °C min^{-1} in N_2 flow (Fig. 3d). $Cu_2(NH_2\text{-}BDC)_2(DABCO)$ is stable up to 245 °C, and demonstrates distinct zones of weight loss commencing at approximately 110–150 °C (3.97% due to the loss of DMF and H_2O. This step of the TGA study (starting at approximately 245 °C) demonstrates the decomposition of linkers (Fig. 3d). The storage capacity of molecules in the pores and channels of MOFs was evaluated using the Brunauer-Emmett-Teller (BET) technique. Based on the findings, the $Cu_2(NH_2\text{-}BDC)_2(DABCO)$ specific surface area was 143.35 ± 3.5 m^2g^{-1}, mesopore diameter at maximum pore volume was 19.568 nm, and total pore volume was 0.629 cm^3 g^{-1}in $Cu_2(NH_2\text{-}BDC)_2(DABCO)$. These results show that the catalyst includes many pores and channels which can be effective in catalytic functions. The average crystal size which has been represented in Fig. 7 based on XRD calculation, was 95.2 nm.

3.2. *Catalytic properties of $Cu_2(NH_2\text{-}BDC)_2(DABCO)$*

To evaluate the catalytic properties of $Cu_2(NH_2\text{-}BDC)_2(DABCO)$ in synthesizing 4H-pyran compounds, the three-component condensations of stoichiometric amounts of dimedone, 4-chlorobenzaldehyde, and malononitrile was studied. The findings data are reported in Table 1. The model reactions were investigated in a variety of solvents, including EtOH, THF, and CH_3CN, using $Cu_2(NH_2\text{-}BDC)_2(DABCO)$ loading of 0.04 g at 75 °C temperature. The use of acetonitrile and tetrahydrofuran solvents resulted in increased reaction time and reduced efficiency; however, using ethanol as a solvent caused reduced reaction time and increased efficiency.

Alpha-lapachone (anti-inflammatory) Beta-lapachone (anticancer, antibacterial)

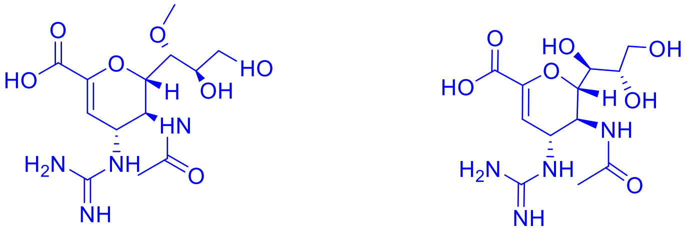

Laninamivir (administered orally) Zanamivir (prevention of influenza)

Scheme 2. Pyran-based natural and synthetic drugs in clinical use [3].

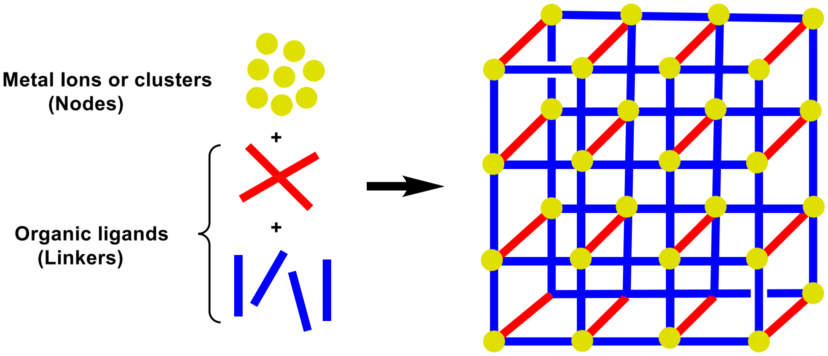

Scheme 3. General scheme of MOF synthesis.

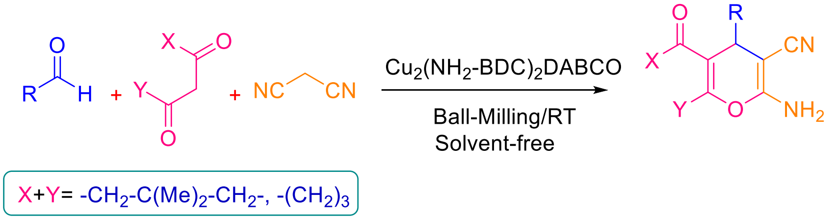

Scheme 4. The heterogeneous catalysis of $Cu_2(NH_2\text{-}BDC)_2(DABCO)$ in a three-component, solvent-free synthesis of 4H-pyran derivatives.

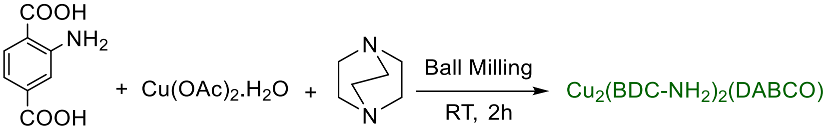

Scheme 5. Ball mill synthesis of $Cu_2(NH_2\text{-}BDC)_2(DABCO)$.

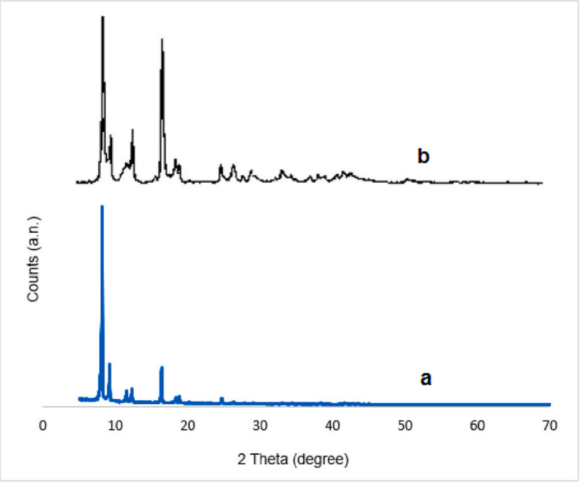

Fig. 1. XRD pattern of **a**) the prepared $Cu_2(NH_2\text{-}BDC)_2(DABCO)$ in this work, **b**) Simulated XRD pattern [42].

It was then examined how temperature affected yield and reaction time. It was shown in Table 1 that low temperatures reduce the efficiency and decrease the reaction speed. The solvent and reaction temperature zoptimization indicated that a higher yield could be achieved in EtOH using a reflux condition over a shorter period. The solvent-free condition has shown that the reaction was carried out

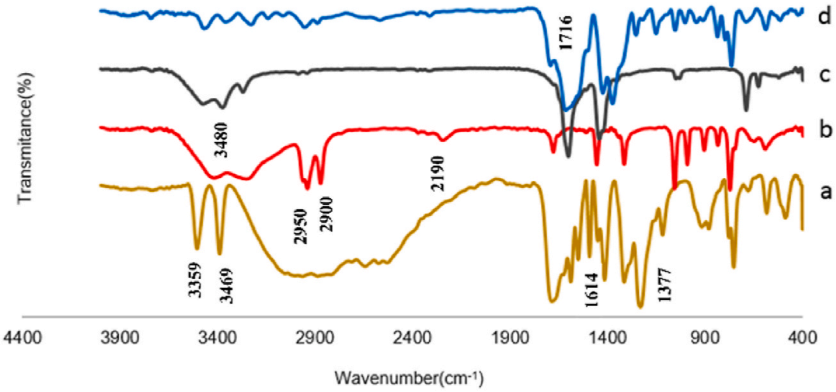

Fig. 2. FT-IR spectra: **a**) 2-aminoterephthalic acid, **b**) DABCO, **c**) $Cu(OAc)_2$, **d**) $Cu_2(NH_2\text{-}BDC)_2(DABCO)$.

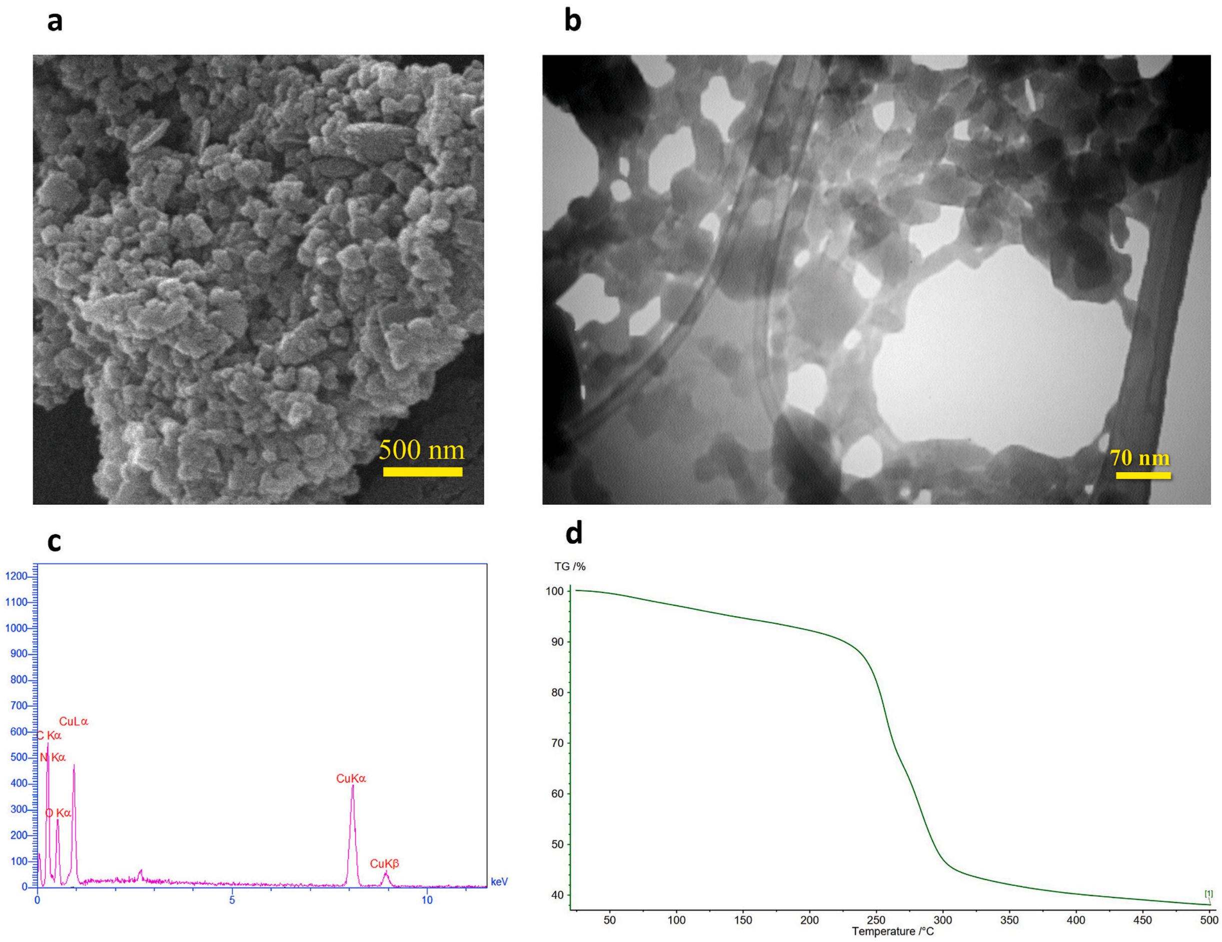

Fig. 3. a) FESEM photographs, b) TEM photographs, c) EDS analysis and d) TGA spectra of $Cu_2(BDC)_2(DABCO)$.

in the shortest possible time and with the highest efficiency (entry 6). The turnover frequency (TOF) of the reaction has been calculated based on the following equation:

$$TOF = \frac{Number\ of\ moles\ of\ reactant\ consumed}{Mole\ of\ catalyst}$$

The TON (Turnover number) indicates the maximum number of molecular reactions or reaction cycles that can occur at a catalyst's

Table 1
Optimizing the three-component reaction of 4-chlorobenzaldehyde (2a), malononitrile (3), and dimedone (4a) under various conditions.

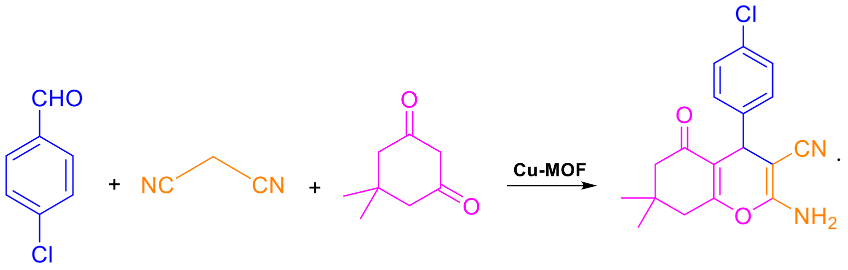

2a **3** **4a** **5a**

Entry	Catalyst loading	Solvent	Temp. (°C)	Time (min)	Yield[b] (%)
1	0.04	THF	75	360	**68**
2	0.04	MeCN	75	300	**85**
3	0.04	EtOH	75	20	**90**
4	0.04	EtOH	50	30	**85**
5	0.04	EtOH	r.t	45	**80**
6	–	Solvent-free	r.t	80	**88**
7	0.02	Solvent-free	r.t	26	**90**
8	0.04	Solvent-free	r.t	5	**96**
9	0.04	Solvent-free	r.t	20	**78**

[a] Conditions of reaction: 4-chlorobenzaldehyde (**2a**, 1.0 mmol), malononitrile (**3**, 1.0 mmol), dimedone (**4a**, 1.0 mmol), grinding, ambient temperature.

[b] Yield refers to isolated products.

reactive centre before the activity of the catalyst begins to degrade. It has been calculated as:

$$TON = TOF\ \left[time^{-1}\right]$$

Based on these equations, for the optimal conditions (Entry 8), the TOF was calculated as 15, and the TON as $5*10^{-2}\ s^{-1}$.

Generally, the ball milling method, except for the purification of the product, if necessary, no solvent is used, and hence it is considered a green synthetic method. Furthermore, the role of catalyst payload on reaction termination was studied. The best and highest yields are obtained with 0.04 g of catalyst (entry 8). The same reaction was performed with $Cu_2(BDC)_2(DABCO)$ as a non-NH_2 catalyst at a relatively higher time and with lower efficiency (entry 9).

To illustrate the extent of the usability of this catalyst, we expanded the zoptimized reaction conditions to various aldehydes and 1,3-cyclohexanedione compounds. Table 2 shows a summary of the findings. As shown in the table, the highest yield was obtained for producing products **5** and **6** under optimal conditions progressively. In addition, the catalyst was simply isolated by filtration and removed from the reaction mixture.

In the next step, ethyl acetoacetate was used as the changeable component for extending the scope of the protocol to the less active reagents. A summary of the data can be found in Table 3. It should be noted that in addition to ethyl acetoacetate, acetylacetone was also studied. Under optimum reaction conditions, the good and desirable yield of the intended products (5, 6, 8, and 9) was achieved within a brief reaction time.

Physical and spectroscopic data were compared to those of previously described compounds in the literature, allowing the clear labelling of all products. In FT-IR spectra of the products, the significant band at around 2190 cm^{-1} is related to the CN stretching band, and the broad band at 3200-3400 cm^{-1} approves the presence of the NH_2 moiety (see Fig. 4d) [50]. As shown in Fig. 5 for the compound **6h**, the characteristic H4 in ^1H NMR spectra of these compounds was appeared as a singlet above 4.0 ppm [50].

A plausible mechanism has been suggested in Scheme 6. The first step consists of forming a cyanocinnamonitrile Knoevenagel intermediate in the reaction of by Cu^{2+}-activated aldehyde reacting with malononitrile. At this stage, the catalyst $Cu_2(NH_2\text{-}BDC)_2(DABCO)$ produces an anion by attacking the acid hydrogens of malononitrile. The produced anion is a nucleophile and attacks the carbonyl group of the aldehyde as an electrophile. Subsequently, by removing a water molecule, the Knoevenagel intermediate is formed. Then, 1,3-dicarbonyl components are added to the intermediate by Michael's addition of the enol form. Then the cyclization, and subsequent tautomerization of the imino-pyran intermediates is carried out on the amino-pyran.

3.3. *Catalytic properties of $Cu_2(NH_2\text{-}BDC)_2(DABCO)$*

The recyclability and the reusability of $Cu_2(NH_2\text{-}BDC)_2(DABCO)$ were also studied for a minimum of six rounds in the model reaction zsynthesizing the product **5a**. A simple filtration process separated the catalyst from the reaction after each run. A summary of the results can be found in Fig. 6. It has been demonstrated that $Cu_2(NH_2\text{-}BDC)_2(DABCO)$ is reusable without a substantial loss of activity in 4H-pyrans synthesis.

XRD and FT-IR techniques were used to zanalyze the structure of the retrieved catalyst, which showed no degradation (Fig. 7a, b,

Table 2
Preparation of 4*H*-pyrans derivatives by using $Cu_2(NH_2\text{-}BDC)_2(DABCO)$ as the catalyst[a]

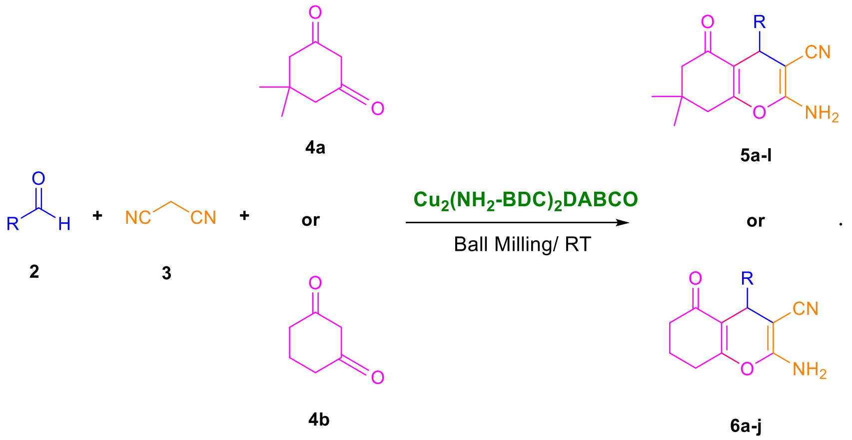

Entry	Aldehyde	Product	Time (min)	Yield (%)[b]	M. P. (°C)	M.P. (°C) [Lit.]
1	4-Chloro benzaldehyde	**5a**	5	96	212–214	212-214 [45]
2	2-Chloro benzaldehyde	**5b**	6	93	209–212	211-213 [46]
3	4- Bromo benzaldehyde	**5c**	8	96	204–207	205-206 [43]
4	Benzaldehyde	**5d**	12	90	223–226	222-224 [44]
5	2-Nitro benzaldehyde	**5e**	9	94	215–218	213-217 [15]
6	3-Nitro benzaldehyde	**5f**	6	90	214–216	216-218 [47]
7	4-Nitro benzaldehyde	**5g**	7	92	180–184	180-182 [48]
8	4-Methyl benzaldehyde	**5h**	20	90	217–220	215-217 [48]
9	3-Hydroxy benzaldehyde	**5i**	23	88	203–206	205-206 [49]
10	4-Hydroxy benzaldehyde	**5j**	25	85	206–209	205-206 [50]
11	2,4-Dichloro benzaldehyde	**5k**	6	94	189–192	192-194 [44]
12	4-Cyano benzaldehyde	**5l**	8	95	220–224	221-224 [50]
13	4-Chloro benzaldehyde	**6a**	20	94	242–244	241-244 [50]
14	2-Chloro benzaldehyde	**6b**	25	90	210–212	210-212 [51]
15	4- Bromo benzaldehyde	**6c**	22	90	235–237	236-238 [52]
16	Benzaldehyde	**6d**	40	86	237–240	241-242 [53]
17	2-Nitro benzaldehyde	**6e**	25	85	198–200	197-199 [54]
18	3-Nitro benzaldehyde	**6f**	30	92	234–237	234-236 [52]
19	4-Nitro benzaldehyde	**6g**	20	88	223–225	222-224 [52]
20	4-Methyl benzaldehyde	**6h**	40	90	224–228	225-226 [44]
21	2,4-Dichloro benzaldehyde	**6i**	23	89	220–223	221-223 [13]
22	4- Hydroxy benzaldehyde	**6j**	42	86	246–248	244-246 [50]

[a] Reaction conditions: aldehyde (**2**, 1.0 mmol), malononitrile (**3**, 1.0 mmol), dimedone or 1,3-cyclohexandione (**4a-b**, 1.0 mmol), $Cu_2(NH_2\text{-}BDC)_2(DABCO)$ (0.04 g), solvent-free and room temperature.

[b] Isolated yield.

and 8a, 8b). The recovered catalyst's FT-IR spectra and x-ray pattern show that its crystalline structure remains intact and stable.

3.4. *Comparison activity of $Cu_2(NH_2\text{-}BDC)_2(DABCO)$*

The new methodology for synthesizing various 4H-pyran derivatives was assessed by comparing several previous reports and accepted methods to demonstrate its efficacy and capabilities. Table 4 provides a comprehensive summary of the results of the present protocol, demonstrating its superiority over other approaches with respect to the yield of the product, reaction time, non-using of organic solvents as green chemistry, as well as simplified separation and reusability of the catalyst.

4. Conclusion

In this paper, we developed a highly effective, environmentally friendly, and greenway for the multicomponent synthesis of 4*H*-pyran derivatives in the presence of $Cu_2(NH_2\text{-}BDC)_2(DABCO)$ as a heterogeneous and renewable catalyst. In addition to all of these, our method has many advantages, such as concise reaction time, the reaction at ambient temperature and non-solvent conditions, high yields of products, as well as easy separation of catalyst from the reaction mixture. It is noteworthy that the catalyst was synthesized in a solvent-free manner.

Table 3
Preparation of 4*H*-pyrans derivatives by using $Cu_2(NH_2\text{-}BDC)_2(DABCO)$ as the catalyst[a]

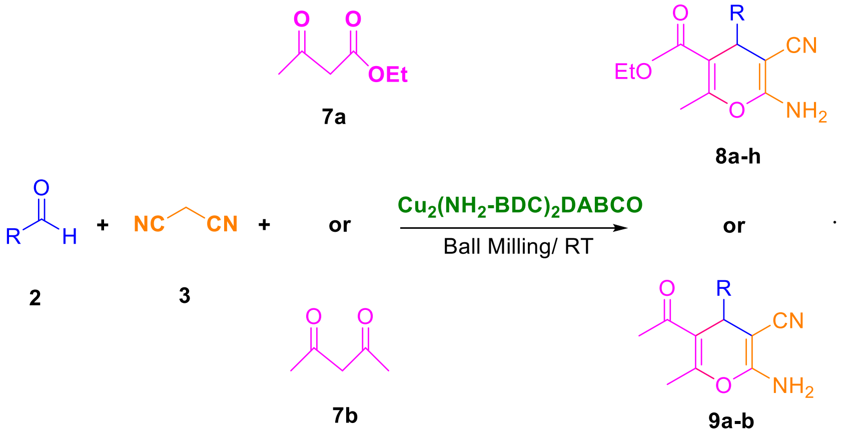

Entry	Aldehyde	Product	Time (min)	Yield (%)[b]	M.P. (°C)	M.P. (°C) [Lit.]
1	4-Chloro benzaldehyde	**8a**	22	92	160–163	162 [55]
2	2-Chloro benzaldehyde	**8b**	25	90	188–192	190-191 [56]
3	4-Bromo benzaldehyde	**8c**	25	92	179–182	179-180 [57]
4	Benzaldehyde	**8d**	60	80	185–188	189 [58]
5	2-Nitro benzaldehyde	**8e**	42	90	178–180	177-178 [57]
6	3-Nitro benzaldehyde	**8f**	40	87	186–190	187-188 [57]
7	4-Nitro benzaldehyde	**8g**	40	89	175–178	174-176 [59]
8	4-Methyl benzaldehyde	**8h**	18	90	173–176	175-176 [59]
9	4-Chloro benzaldehyde	**9a**	30	65	149–154	153-155 [60]
10	3-Nitro benzaldehyde	**9b**	42	63	160–164	166 [61]

[a] Reaction conditions: aldehyde (**2**, 1.0 mmol), malononitrile (**3**, 1.0 mmol), acetyl acetone or ethyl acetoacetate (**7a-b,** 1.0 mmol), $Cu_2(NH_2\text{-}BDC)_2(DABCO)$ (0.04 g), solvent-free and room Temperature.

[b] Isolated yield.

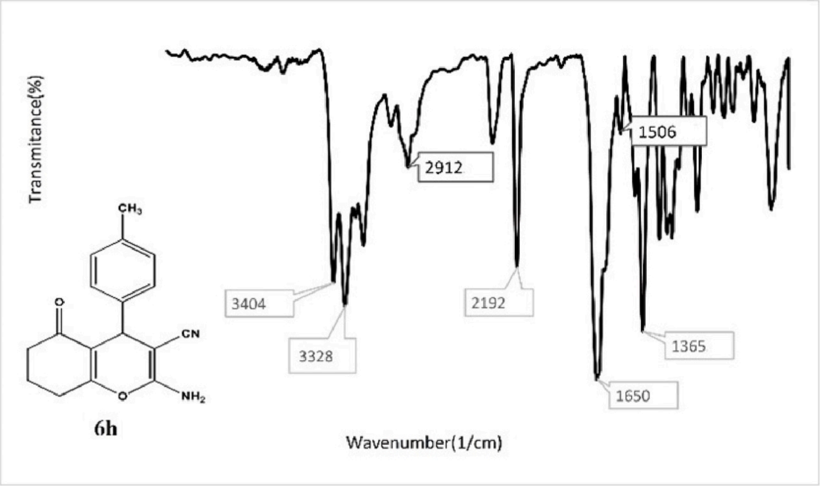

Fig. 4. FT-IR spectra of 2-amino-3-cyano-4-(4-methylphenyl)-5-oxo-5,6,7,8-tetrahydro-4H-1-benzopyran (**6h**).

Author contribution statement

Zahra Akhlaghi, Mohammad R. Naimi-Jamal, Leila Panahi: Conceived and designed the experiments; Performed the experiments; Analyzed and interpreted the data; Contributed reagents, materials, analysis tools or data; Wrote the paper.

Mohammad G. Dekamin: Conceived and designed the experiments; Contributed reagents, materials, analysis tools or data.

Bahareh Farasati Far: Analyzed and interpreted the data; Wrote the paper.

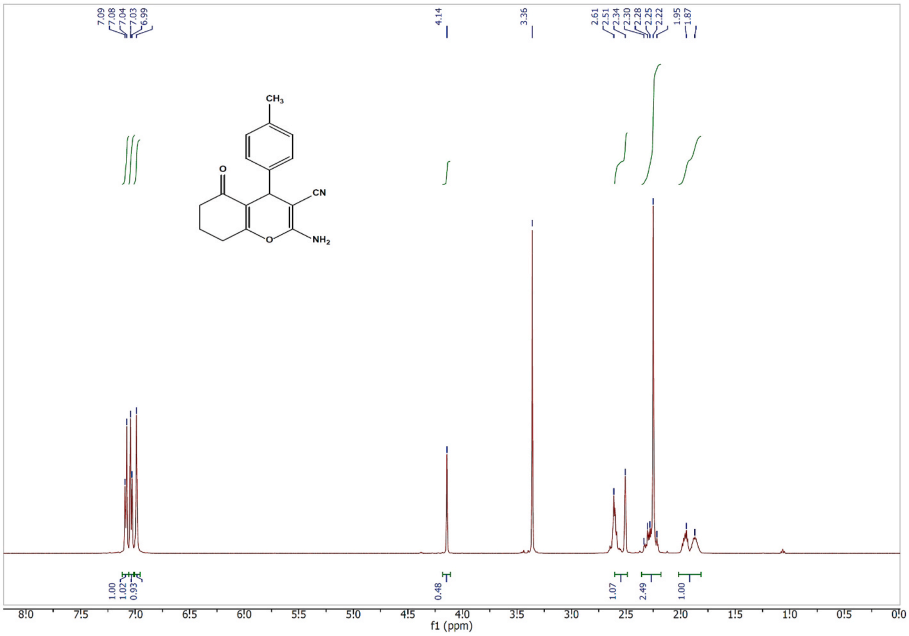

Fig. 5. ^{1}H NMR spectra of 2-amino-3-cyano-4-(4-*methyl*phenyl)-5-oxo-5,6,7,8-tetrahydro-4H-1-benzopyran (**6h**).

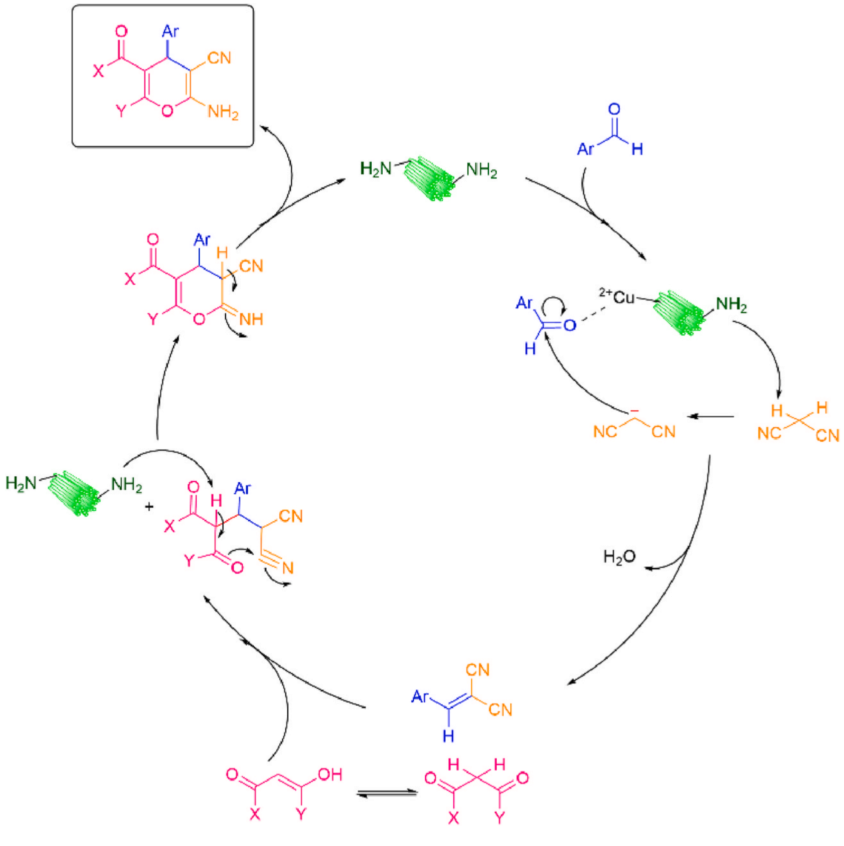

Scheme 6. The suggested mechanism of the 4*H*-pyrans derivatives synthesis using $Cu_2(NH_2\text{-}BDC)_2(DABCO)$.

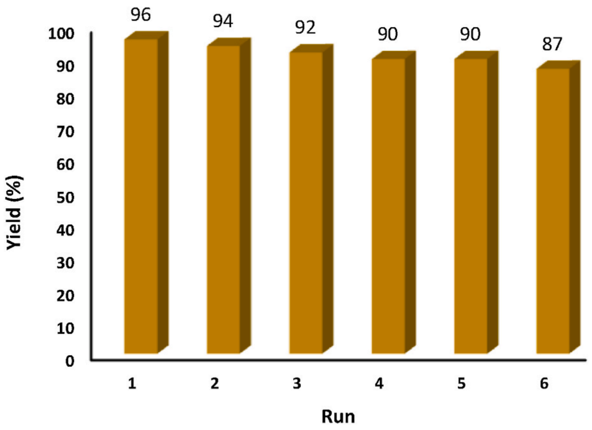

Fig. 6. Reusability of $Cu_2(NH_2\text{-}BDC)_2(DABCO)$ catalyst for the MCR synthesis of 4*H*-pyran **5a**.

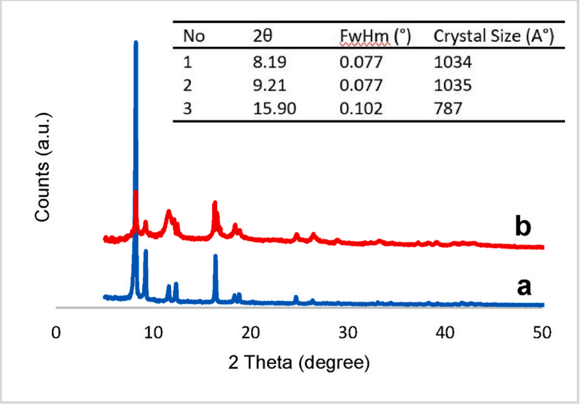

No	2θ	FwHm (°)	Crystal Size (A°)
1	8.19	0.077	1034
2	9.21	0.077	1035
3	15.90	0.102	787

Fig. 7. X-ray diffraction of powder of $Cu_2(NH_2\text{-}BDC)_2(DABCO)$: a) Fresh catalyst, b) Recovered catalyst after 6th runs.

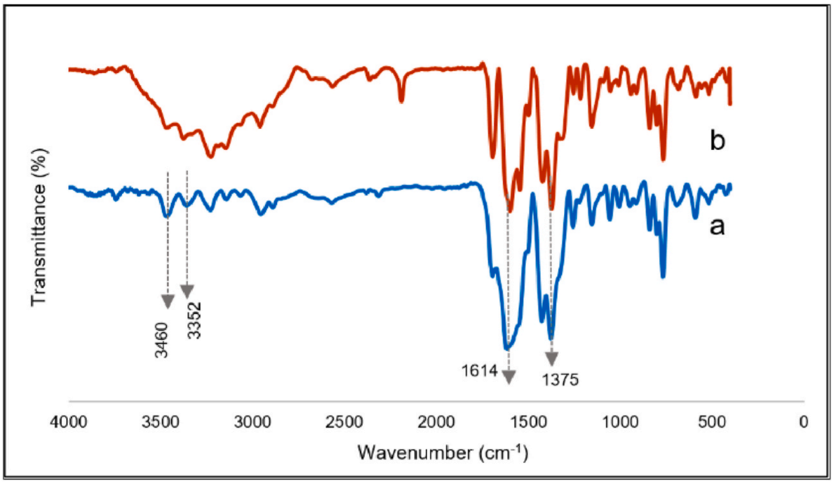

Fig. 8. FT-IR spectra of powder of $Cu_2(NH_2\text{-}BDC)_2(DABCO)$: **a**) Fresh catalyst, **b**) Recovered catalyst after 6th runs.

Table 4
A comparison of the previously reported procedures for the synthesis of chemicals **5a**, **6f**, and **8a**.

Entry	Product	Catalyst	Catalyst loading	Solvent	Temp. (°C)	Time (min)	Yield (%)	Ref.
1	**5a**	$Cu_2(NH_2\text{-BDC})_2(DABCO)$	40 mg	Solvent-free	r.t	5	96	This work
2	**5a**	$Cu_2(BDC)_2(DABCO)$	40 mg	Solvent-free	r.t	20	78	This work
3	**5a**	$NH_4Al(SO_4)_2.12H_2O$ (Alum)	20 mg	EtOH	80	120	94	[62]
4	**5a**	$PhB(OH)_2$	5 mol%	H_2O/EtOH	Reflux	30	84	[63]
5	**5a**	SiO_2-Pr-SO3H	30 mg	H_2O/EtOH	Reflux	15	97	[17]
6	**5a**	KF/Al_2O_3	250 mg	DMF	r.t	60–180	48	[60]
7	**5a**	MPA-MDAZY[b]	140 mg	EtOH	80	70	90	[64]
8	**5a**	ChCl/Urea DES[c]	1 mL	ChCl/Urea DES[c]	80	60–240	92	[65]
9	**5a**	Amberlyst A21	30 mg	EtOH	r.t	60	84	[66]
10	**6f**	Sodium Alginate	10 mol%	EtOH	Reflux	52	93	[67]
11	**6f**	MPA-MDAZY[b]	140 mg	EtOH	80	40	75	[64]
12	**6f**	Lipase from Porcine pancreas (PPL)	30 mg	H_2O/EtOH	35	60	96	[68]
13	**8a**	ChCl/Urea DES[c]	1 mL	ChCl/Urea DES[c]	80	210	82	[65]
14	**8a**	Sodium Alginate	10 mol%	EtOH	Reflux	150	90	[67]
15	**8a**	nanocrystalline ZnO	10 mol%	H_2O/EtOH	r.t	150	96	[61]

[a] Entries **1–8**: Obtained outcomes for the synthesis of molecule**5a**, Entries **9–11**: Obtained outcomes for the synthesis of molecule**6f**, Entries **12–14**: Obtained findings for **8a** compound synthesis.

[b] 12-Molybdophosphoric acid (MPA), modified dealuminated zeolite Y (MDAZY).

[c] Deep eutectic solvent (DES).

Funding statement

Partial support by the Iran University of Science and Technology is acknowledged.

Data availability statement

Data will be made available on request.

Declaration of interest's statement

The authors declare no conflict of interest.

References

[1] O.V. Drygina, A.D. Garnovskii, 4H-pyrans, Chem. Heterocycl. Compd. 19 (1983) 807–821.

[2] O.V. Drygina, A.D. Garnovskii, A.V. Kazantsev, 2H-pyrans, Chem. Heterocycl. Compd. 21 (1985) 239–253.

[3] D. Kumar, P. Sharma, H. Singh, K. Nepali, G.K. Gupta, S.K. Jain, F. Ntie-Kang, The value of pyrans as anticancer scaffolds in medicinal chemistry, RSC Adv. 7 (2017) 36977–36999.

[4] Ch Narajji, M.D. Karvekar, A.K. Das, Synthesis and antioxidant activity of 1,2-Bis(1-ethyl-2-substitutedphenylindolizin-3-yl)diselane, Asian J. Chem. 20 (2008) 6183–6188.

[5] J. Skommer, D. Wlodkowic, M. Mättö, M. Eray, J. Pelkonen, HA14-1, a small molecule Bcl-2 antagonist, induces apoptosis and modulates action of selected anticancer drugs in follicular lymphoma B cells, Leuk. Res. 30 (2006) 322–331.

[6] S.J. Mohr, M.A. Chirigos, F.S. Fuhrman, J.W. Pryor, Pyran copolymer as an effective adjuvant to chemotherapy against a murine leukemia and solid tumor, Cancer Res. 35 (1975) 3750–3754.

[7] H.W. Jie, L.Z. Zhang, Á.Á. Malononitrile, Highly efficient three-component , one-pot synthesis of dihydropyrano [3,2-c] chromene derivatives, Monatsh. Chem. 141 (2010) 1107–1112.

[8] R. Kumar, M. Yusuf, Chromones and bischromones: an account of photoinduced reactions, Arkkitehti (2006) 239–264.

[9] H. Aghahosseini, A. Ramazani, Magnetite L-proline as a reusable nano-biocatalyst for efficient synthesis of 4H-benzo[b]pyrans in water: a green protocols, Eurasian Chem. Commun. 2 (3) (2020) 410–419.

[10] B. Baghernejad, M. Fiuzat, A new strategy for the synthesis of 2-amino-4H-pyran derivatives in aqueous media using DABCO-CuCl complex as a novel and efficient catalyst, Eurasian Chem. Commun. 2 (11) (2020) 1088–1092.

[11] J. Zheng, Y. Li, One-pot synthesis of tetrahydrobenzo [b] pyran and dihydropyrano [c] chromene derivatives in aqueous media by using trisodium citrate as a green catalyst, Arch. Appl. Sci. Res. 3 (2011) 381–388.

[12] V.T. Kamble, M. Sadaf, B.S. Samer, Highly efficient synthesis of tetrahydrobenzo[b]pyrans promoted by cesium carbonate under visible light, Iran. Chem. Commun. 5 (2017) 167–172.

[13] B. Baghernejad, Application of ninhydrin as an efficient and novel catalyst for the preparation of 2-amino-4H-pyran derivatives, J. Appl. Organomet. Chem. 1 (1) (2021) 17–21.

[14] H. Hu, F. Qiu, A. Ying, J. Yang, H. Meng, An environmentally benign protocol for aqueous synthesis of tetrahydrobenzo[b]pyrans catalysed by cost-effective ionic liquid, Int. J. Mol. Sci. 15 (2014) 6897–6909.

[15] F. Shirini, M.S.N. Langarudi, N. Daneshvar, Preparation of a new DABCO-based ionic liquid $[H_2\text{-DABCO}][H_2PO_4]_2$} and its application in the synthesis of tetrahydrobenzo[b]pyran and pyrano[2,3-d]pyrimidinone derivatives, J. Mol. Liq. 234 (2017) 268–278.

[16] N. Hazeri, M. Maghsoodlou T, F. Mir, M. Kangani, H. Saravani, E. Molashahi, An efficient one-pot three-component synthesis of tetrahydrobenzo[b]pyran and 3,4-dihydropyrano[c]chromene derivatives using starch solution as catalyst, Chin. J. Catal. 35 (2014) 391–395.

[17] G. Ziarani, A. Abbasi, A. Badiei, Z. Aslani, An efficient synthesis of tetrahydrobenzo[b]pyran derivatives using sulfonic acid functionalized silica as an efficient catalyst, E-Journal Chem. 8 (2011) 293.

[18] F.K. Behbahani, M. Naderi, One-pot synthesis of 2-amino-4H-chromenes catalysed by Fe(ClO4)3/SiO2, Russ. J. Gen. Chem. 86 (2016) 2804–2806.

[19] M. Abdollahi-Alibeik, N. Sadeghi-Vasafi, A. Moaddeli, A. Rezaeipoor-Anari, ClO_4^-/Al-MCM-41 nanoparticles as a solid acid catalyst for the synthesis of 2-amino-3-cyanopyridines, Res. Chem. Intermed. 42 (2016) 2867–2881.
[20] J. Albadi, A. Mansournezhad, Poly (4-vinylpyridine) efficiently catalysed one-pot four-component synthesis of pyrano [2, 3-c] pyrazoles, Curr. Chem. Lett. 3 (2014) 221–227.
[21] S. Gaikwad, M.V.B. Unnamatla, Simple, highly efficient synthesis 2-Amino-4-Phenyl-4,5,6,7-Tetrahydropyrano[3,2-c]Carbazole-3-Carbonitrile derivatives using silica supported dodeca-tungstophosphoric acid DTP/SiO_2, J. Appl. Organomet. Chem. 2 (1) (2022) 24–30.
[22] a) J.L.C. Rowsell, O.M. Yaghi, Metal-organic frameworks: a new class of porous materials, Microporous Mesoporous Mater. 73 (2004) 3–14;
b) H.C. Zhou, K. Susumu, Metal–organic frameworks (MOFs), Chem. Soc. Rev. 43 (2014) 5415–5418.
[23] C.A. Fernandez, S.K. Nune, R.K. Motkuri, P.K. Thallapally, C. Wang, J. Liu, G.J. Exarhos, B.P. McGrail, Synthesis, characterisation, and application of metal organic framework nanostructures, Langmuir 26 (2010) 18591–18594.
[24] A. Schoedel, M. Li, D. Li, M. O'Keeffe, O.M. Yaghi, Structures of metal-organic frameworks with rod secondary building units, Chem. Rev. 116 (2016) 12466–12535.
[25] M. Kurmoo, Magnetic metal–organic frameworks, Chem. Soc. Rev. 38 (2009) 1353.
[26] J.E. Mondloch, O. Karagiaridi, O.K. Farha, J.T. Hupp, Activation of metal – organic framework materials, CrystEngComm 15 (2013) 9258–9264.
[27] L. Sarkisov, R.L. Martin, M. Haranczyk, B. Smit, On the flexibility of metal-organic frameworks, J. Am. Chem. Soc. 136 (2014) 2228–2231.
[28] H.C. Zhou, J.R. Long, O.M. Yaghi, Introduction to metal-organic frameworks, Chem. Rev. 112 (2012) 673–674.
[29] A. Aijaz, Q. Xu, Catalysis with metal nanoparticles immobilised within the pores of metal − organic frameworks, J. Phys. Chem. Lett. 5 (2014) 1400–1411.
[30] B. Manna, S. Mukherjee, A.V. Desai, S. Sharma, R. Krishna, S.K. Ghosh, A π-electron deficient diaminotriazine functionalised MOF for selective sorption of benzene over cyclohexane, Chem. Commun. 51 (2015) 15386–15389.
[31] A. Corma, H. García, F.X. Llabrés i Xamena, Engineering metal organic frameworks for heterogeneous catalysis, Chem. Rev. 110 (2010) 4606–4655.
[32] J.B. Decoste, G.W. Peterson, Metal−Organic frameworks for air purification of toxic chemicals, Chem. Rev. 114 (2014) 5695–5727.
[33] V. Safarifard, S. Beheshti, A. Morsali, An interpenetrating amine-functionalised metal-organic framework as an efficient and reusable catalyst for the selective synthesis of tetrahydro-chromenes, CrystEngComm 17 (2015) 1680–1685.
[34] M. Giménez-Marqués, T. Hidalgo, C. Serre, P. Horcajada, Nanostructured metal-organic frameworks and their bio-related applications, Coord. Chem. Rev. 307 (2015) 342–360.
[35] J. Li, J. Sculley, H. Zhou, Metal organic frameworks for separations, Chem. Rev. 112 (2012) 869–932.
[36] N.C. Burtch, H. Jasuja, K.S. Walton, Water stability and adsorption in metal − organic frameworks, Chem. Rev. 114 (2014) 10575–10612.
[37] M. Zhang, C. Chen, Q. Wang, W. Fu, K. Huang, W. Zhou, A metal–organic framework functionalised with piperazine exhibiting enhanced CH_4 storage, J. Mater. Chem. A. 5 (2017) 349–354.
[38] K. Lee, W.C. Isley, A.L. Dzubak, P. Verma, S.J. Stoneburner, L. Lin, J.D. Howe, E.D. Bloch, D.A. Reed, M.R. Hudson, C.M. Brown, R. Long, B. Neaton, B. Smit, C. J. Cramer, D.G. Truhlar, L. Gagliardi, Design of a metal − organic framework with enhanced back bonding for separation of N_2 and CH_4, J. Am. Chem. Soc. 136 (2013) 698–704.
[39] J. Chun, S. Kang, N. Park, E.J. Park, X. Jin, K. Kim, H.O. Seo, S.M. Lee, H.J. Kim, W.H. Kwon, Y. Park, J.M. Kim, Y.D. Kim, S.U. Son, Metal−Organic Framework@Microporous organic network: hydrophobic adsorbents with a crystalline inner porosity, J. Am. Chem. Soc. 136 (2014) 6786–6789.
[40] M.P. Suh, H.J. Park, T.K. Prasad, D. Lim, Hydrogen storage in metal organic frameworks, Chem. Rev. 112 (2011) 782–835.
[41] a) R.M. Claramunt, C. Lopez, D. Sanz, J. Elguero, Mechano heterocyclic chemistry: grinding and ball mills, Adv. Heterocycl. Chem. 112 (2014) 117–143;
b) S. Mahdian, M.R. Naimi-Jamal, L. Panahi, Activity of $M_2(BDC)_2$(DABCO) (M= Co, Ni, Cu and Zn) metal-organic frameworks prepared via ball-milling solvent-free method in acylation of alcohols, amines and aldehydes, ChemistrySelect 3 (2018) 11223–11229;
c) H. Cheng, J.G. Hernández, C. Bolm, Mechanochemical cobalt-catalyzed C−H bond functionalizations by ball milling, Adv. Synth. Catal. 360 (2018) 1800–1804;
d) Z. Liu, H. Xu, G.W. Wang, Palladium-catalyzed ortho-halogenations of acetanilides with N-halosuccinimides via direct sp^2 C–H bond activation in ball mills, Beilstein J. Org. Chem. 14 (2018) 430–435.
[42] a) M.A. Alavi, A. Morsali, S.W. Joo, B.K. Min, Ultrasound and modulation assisted synthesis of {[$Cu_2(BDC\text{-}NH_2)_2$(dabco)]DMF.3H_2O} nanostructures; New precursor to prepare nanorods and nanotubes of copper(II) oxide, Ultrason. Sonochem. 22 (2015) 349–358;
b) L. Panahi, M.R. Naimi-Jamal, J. Mokhtari, Ultrasound-assisted Suzuki-Miyaura reaction catalysed by Pd@$Cu_2(NH_2\text{-}BDC)_2$(DABCO, J. Organomet. Chem. 868 (2018) 36–46;
c) M.R. Naimi-Jamal, S. Mashkouri, A. Sharifi, An efficient, multicomponent approach for solvent-free synthesis of 2-amino-4H-chromene scaffold, Mol. Divers. 14 (2010) 473–477;
d) M. Amirnejad, M.R. Naimi-Jamal, H. Tourani, H. Ghafuri, A facile solvent-free one-pot three-component method for the synthesis of 2-amino-4H-pyrans and tetrahydro-4H-chromenes at ambient temperature, Monatsh. Chem. 144 (2013) 1219–1225.
[43] N.O. Mahmoodi, Z. Khazaei, Preparation, characterisation and use of sulfonylbis(1,4-phenylene)bis(sulfamic acid) as an eco-benign, efficient, reusable and heterogeneous catalyst for the synthesis of mono- and bis-chromenes, J. Iran. Chem. Soc. 14 (2017) 1889–1898.
[44] H. Kiyani, F. Ghorbani, Efficient tandem synthesis of a variety of pyran-annulated heterocycles, 3,4-disubstituted isoxazol-5(4H)-ones, and α,β-unsaturated nitriles catalysed by potassium hydrogen phthalate in water, Res. Chem. Intermed. 41 (2015) 7847–7882.
[45] A.G. Mulik, D.R. Chandam, D.R. Patil, P.P. Patil, G.N. Mulik, S.T. Salunkhe, M.B. Deshmukh, Protic ionic liquids: a lucid, rational tool for synthesis of phthalazinediones, quinoxalines and benzopyrans, Res. Chem. Intermed. 41 (2015) 10085–10096.
[46] E. Tabrizian, A. Amoozadeh, A unique approach to magnetisation of metal oxides: nano-Fe_3O_4@TDI@TiO_2 as a highly efficient, magnetically separable and recyclable heterogeneous nanocatalyst, Catal. Sci. Technol. 6 (2016) 6267–6276.
[47] A. Ahad, M. Farooqui, Organocatalyzed domino reactions: diversity oriented synthesis of pyran-annulated scaffolds using in situ-developed benzylidenemalononitriles, Res. Chem. Intermed. 43 (2017) 2445–2455.
[48] M.A. Zolfigol, M. Yarie, S. Baghery, [4,4′-Bipyridine]-1,1′-diium tricyanomethanide as a nanostructured molten salt and its catalytic application in the synthesis of tetrahydrobenzo[b]pyrans, amido and aminoalkyl naphthol derivatives, J. Mol. Liq. 222 (2016) 923–932.
[49] R.-Y. Guo, Z.-M. An, L.-P. Mo, R.-Z. Wang, H.-X. Liu, S.-X. Wang, Z.-H. Zhang, Meglumine: a novel and efficient catalyst for one-pot, three-component combinatorial synthesis of functionalised 2-amino-4 H-pyrans, ACS Comb. Sci. 15 (2013) 557–563.
[50] O.H. Qareaghaj, S. Mashkouri, M.R. Naimi-Jamal, G. Kaupp, Ball milling for the quantitative and specific solvent-free Knoevenagel condensation + Michael addition cascade in the synthesis of various 2- amino-4-aryl-3-cyano-4H-chromenes without heating, RSC Adv. 4 (2014) 48191–48201.
[51] R.M.N. Kalla, A. Varyambath, M.R. Kim, I. Kim, Amine-functionalized hyper-crosslinked polyphenanthrene as a metal-free catalyst for the synthesis of 2-amino-tetrahydro-4H-chromene and pyran derivatives, Appl. Catal. Gen. 538 (2017) 9–18.
[52] C.S. Maheswari, R. Ramesh, A. Lalitha, Synthesis, characterization, and catalytic behavior of bamboo rice husk ash, J. Chin. Chem. Soc. 64 (2017) 889–895.
[53] W.-B. Sun, P. Zhang, J. Fan, S.-H. Chen, Z.-H. Zhang, Lithium bromide as a mild, efficient, and recyclable catalyst for the one-pot synthesis of tetrahydro-4 H -chromene derivatives in aqueous media, Synth. Commun. 40 (2010) 587–594.
[54] M. Nasr-Esfahani, T. Abdizadeh, Nanorod vanadatesulfuric acid as a novel, recyclable and heterogeneous catalyst for the one-pot synthesis of tetrahydrobenzopyrans, J. Nanosci. Nanotechnol. 13 (2013) 5004–5011.
[55] K.D. Khalil, H.M. Al-Matar, Chitosan based heterogeneous catalyses: chitosan-grafted-poly(4- Vinylpyridne) as an efficient catalyst for michael additions and alkylpyridazinyl carbonitrile oxidation, Molecules 18 (2013) 5288–5305.
[56] Z. Li, A. Zhu, J. Yang, One-Pot three-component mild synthesis of 2-Aryl-3-(9-alkylcarbazol-3-yl)thiazolin-4-ones, J. Heterocycl. Chem. 49 (2012) 1458–1461.
[57] B. Maleki, S. Sheikh, One-pot synthesis of 2-Amino-2-chromene and 2-Amino-3-cyano-4H-pyran derivatives promoted by potassium fluoride, Org. Prep. Proced. Int. 47 (2015) 368–378.

[58] M. Gupta, M. Gupta, R. Rajnikant, V.K. Gupta, Salicyldimine-based Schiff's complex of copper(II) as an efficient catalyst for the synthesis of nitrogen and oxygen heterocycles, New J. Chem. 39 (2015) 3578–3587.

[59] B. Maleki, M. Baghayeri, Abadi S.A. Jannat, R. Tayebee, A. Khojastehnezhad, Ultrasound promoted facile one pot synthesis of highly substituted pyran derivatives catalysed catalryzed by silica-coated magnetic $NiFe_2O_4$ nanoparticle-supported $H_{14}[NaP_5W_{30}O_{110}]$ under mil, RSC Adv. 6 (2016) 96644–96661.

[60] X.-S. Wang, D.-Q. Shi, S.-J. Tu, C.-S. Yao, A convenient synthesis of 5-Oxo-5,6,7,8-tetrahydro-4H-benzo-[b]-pyran derivatives catalyzed by KF-alumina, Synth. Commun. 33 (2003) 119–126.

[61] P. Bhattacharyya, K. Pradhan, S. Paul, A.R. Das, Nano crystalline ZnO catalysed one pot multicomponent reaction for an easy access of fully decorated 4H-pyran scaffolds and its rearrangement to 2-pyridone nucleus in aqueous media, Tetrahedron Lett. 53 (2012) 4687–4691.

[62] A.A. Mohammadi, M.R. Asghariganjeh, A. Hadadzahmatkesh, Synthesis of tetrahydrobenzo[b]pyran under catalysis of $NH_4Al(SO_4)_2{\cdot}12H_2O$ (Alum), Arab. J. Chem. 10 (2017) S2213–S2216.

[63] M. Ghashang, S.S. Mansoor, K. Aswin, S.P.N. Sudhan, Poly(4-vinylpyridinium)hydrogensulfate as an efficient and convenient catalyst for a three-component synthesis of 7-methyl-10-aryl-10H-5,8-dioxa-benzo[b]fluoren-9,11-diones, Res. Chem. Intermed. 41 (2015) 5239–5251.

[64] S.F. Hojati, M. Moosavifar, T. Ghorbanipoor, Improvement in nanocomposite host (nanocavity of dealuminated zeolite Y)-guest (12-molybdophosphoric acid) catalytic activity and its application to the one-pot three-component synthesis of tetrahydrobenzo[b]pyrans, Compt. Rendus Chem. 20 (2017) 520–525.

[65] N. Azizi, S. Dezfooli, M. Khajeh, M.M. Hashemi, Efficient deep eutectic solvents catalysed synthesis of pyran and benzopyran derivatives, J. Mol. Liq. 186 (2013) 76–80.

[66] M. Bihani, P.P. Bora, G. Bez, H. Askari, Amberlyst A21: a reusable solid catalyst for green synthesis of pyran annulated heterocycles at room temperature, Compt. Rendus Chem. 16 (2013) 419–426.

[67] M.G. Dekamin, S.Z. Peyman, Z. Karimi, S. Javanshir, M.R. Naimi-Jamal, M. Barikani, Sodium alginate: an efficient biopolymeric catalyst for green synthesis of 2-amino-4H-pyran derivatives, Int. J. Biol. Macromol. 87 (2016) 172–179.

[68] J.C. Xu, W.M. Li, H. Zheng, Y.F. Lai, P.F. Zhang, One-pot synthesis of tetrahydrochromene derivatives catalysed by lipase, Tetrahedron 67 (2011) 9582–9587.